Global Lineaments: Application of Digital Terrain Modelling

Igor V. FLORINSKY

Abstract

In the past few decades, there have been proposals suggesting that hidden global linear (helical) structures exist, which are tectonically and topographically expressed. In this study, this hypothesis was checked using digital terrain modelling. The study was based on a 30 arc-minute gridded global digital elevation model. Eighteen topographic variables were for the first time calculated and mapped for the entire surface of the Earth. Digital terrain analysis provided support for the existence of global lineaments: on maps of specific catchment area, it was possible to detect five mutually symmetrical pairs of helical structures encircling the Earth from pole to pole. The structures are topographically expressed by patterns of the global ridge network. They are apparently associated with traces of the torsional deformation of the planet: two double helices are in reasonable agreement with theoretically predicted traces of shear fractures, while another two double helices are in reasonable agreement with ideal traces of cleavage cracks. Geological phenomena observed along the structures are discussed (i.e. fracturing, faults, crystal, and ore deposits). It is probable that double helices are relict structures similar to a planetary network of helical lineaments on Venus.

Keywords: tectonics, geological structure, catchment area, helix, planet.

1 Introduction

Lineaments are commonly recognized as linear surface manifestations of geological features of various origin, age, depth, and size (Hobbs 1904, O'Leary *et al.* 1976, Makarov 1981). They are usually associated with fracture zones, faults, folds, other linear features, and their sequences. Lineaments, as a rule, are topographically expressed, and can be observed on maps and remotely sensed images at a wide range of scales. At a regional scale, one can treat lineaments geometrically as planar straight

lines. At continental and global scales, they should be considered as spatial curves.

Much attention has been paid to planetary systems of lineaments. There have been three groups of investigations: (a) detection of regularities in the global distribution and direction of lineaments by analysing physiographic and geological maps and then developing models for the regularities observed (Chebanenko 1963, Moody 1966, Katterfeld and Charushin 1973, Besprozvanny *et al.* 1994); (b) development of a physical-mathematical model of a global tectonic process causing an ideal planetary network of lineaments and then comparison of the ideal and actual lineament networks (Vening Meinesz 1947, Dolitsky and Kiyko 1963, Chebanenko and Fedorin 1983); and (c) laboratory simulation of a global lineament network using rotatable spheres (Knetsch 1965, Cherednichenko *et al.* 1966). The origin of global lineament systems was usually associated with rotation-derived forces.

Rance (1968) developed a physical-mathematical model of the torsional deformation of a sphere. The torsion was attributed to an action of possible mantle convection currents on the crust. According to the model, there are two systems of traces of torsional failure surfaces on the surface of the sphere: shear fractures and cleavage cracks (Rance 1967). Geometrically, traces of torsional deformation constitute two systems of double helices encircling the sphere from pole to pole (Figure 1a). The traces vary in inclination at the equator: pairs of mutually symmetrical helices tracing shear fractures are inclined at 15° to 18° and 165° to 162°, and other pairs of helices tracing cleavage cracks are inclined at 56° to 62° and 124° to 118°. A search for actual global helical tectonic features resulted in the detection of several relatively small lineaments referring to faults, trenches, ridges, fracture zones, and seamount chains in basins of the Pacific and Indian Oceans (Rance 1967, Rance 1969).

O'Driscoll (1980) detected two global topographically and tectonically expressed double helical zones by a visual analysis of physiographic maps. The zones had the same inclination at the equator: about 32° and 160° (Figure 1b). O'Driscoll believed that these are fundamental structural belts governing the global deformation network and the planetary evolution. Volkov (1995) reported six global double helical structures also detected by a visual analysis of physiographic maps. At the equator, three of them were inclined at about 12° and 168°, and the other three structures were inclined at about 22° and 158° (Figure 1c). Volkov presumed that these are traces of tidal effects within the Earth-Moon resonance system of past ages.

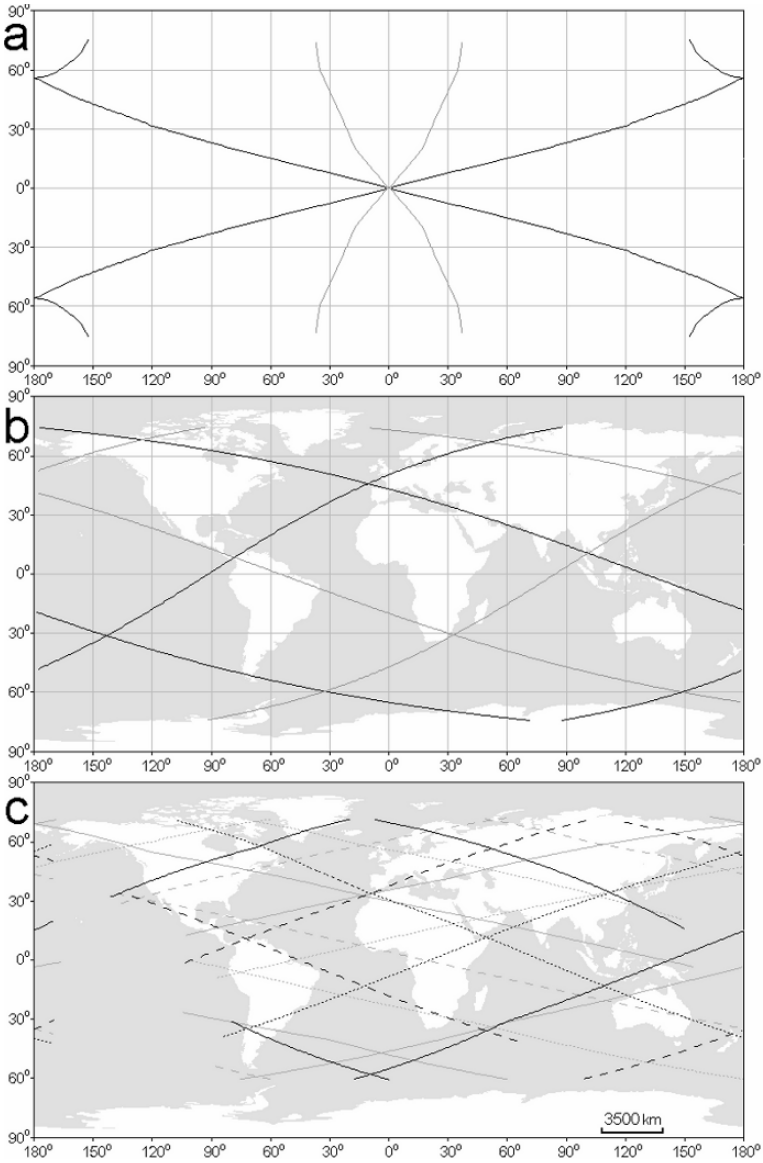

Figure 1. Global helices. (a) Theoretical traces of torsional deformation (Rance 1967): shear fractures (black) and cleavage cracks (grey). (b) Axes of double helical zones (O'Driscoll 1980). (c) Six double helices (Volkov 1995): lines of different style show different structures. The Mercator projection was originally used. The Plate Carrée projection is used here.

Although much attention has been paid to global lineaments, their existence is still questionable. This is because of (1) the qualitative character of

topographic, physiographic, and geological maps analysed in previous works; (2) inaccurate presentation of seafloor bathymetry on those maps produced before reasonably accurate bathymetric data became available; (3) impossibility of considering all natural conditions in a mathematical model; (4) obvious differences between the Earth's rotation and its laboratory simulation; and (5) a basic conflict between the plate tectonic theory and the possibility of the existence of global topographic and tectonic structures.

Technical flaws can be obviated using quantitative descriptions of global topography, a digital elevation model (DEM), and methods of digital terrain modelling (Moore *et al.* 1991, Florinsky 1998a). Topography, resulting from the interaction of endogenous and exogenous geophysical processes of different spatial and temporal scales, carries information on both surface processes and tectonic features. Thus, if global helical structures really exist, there is a good chance that they are manifested in relief.

DEMs have been used to detect lineaments at regional scales (Schowengerdt and Glass 1983, Florinsky 1996, Chorowicz *et al.* 1999) and continental scales (Moore and Simpson 1983, Florinsky 2005). Although some phenomena have been modelled and explored with DEMs at the global scale, such as mantle convection (Cazenave *et al.* 1989), the Earth's crust (Mooney *et al*. 1998), hydrological processes (Coe 1998, Renssen and Knoop 2000), and statistical characteristics of relief (McClean and Evans 2000, Vörösmarty *et al*. 2000, Kazanskii 2005), DEMs have not been used to study global lineaments. In this chapter, hidden, topographically expressed global lineaments are detected and interpreted using methods of digital terrain modelling.

2 Materials and Methods

The study was based on a 30 arc-minute gridded global DEM assembled from several sources. Elevations of the land topography were derived from GLOBE, the 30 arc-second gridded global DEM (GLOBE Task Team 1999). Most of the seafloor topography was taken from ETOPO2, the 2 arc-minute gridded global DEM (U.S. Department of Commerce 2001). Bathymetry of the Antarctic Continental Shelf, Caspian Sea, and some large lakes was digitised using topographic maps. The DEM consisted of 721 columns by 361 rows. For Antarctica and Greenland, GLOBE includes elevations of ice surfaces rather than subglacial topography (Hastings and Dunbar 1998). These areas were included in the DEM to retain a united configuration of data.

Global DEMs include high frequency noise (Coe 1998, Hastings and Dunbar 1998, Arabelos 2000) leading to the derivation of useless, noisy digital models and unreadable maps of secondary topographic variables (Florinsky 2002). The problem can be partially resolved by DEM smoothing. To denoise the DEM, one, two, and three iterations of smoothing were applied to the DEM using a 3 × 3 kernel with linear inverse distance weights.

This study was the first application of digital terrain modelling to reveal lineaments at the global scale. Topographic attributes *a priori* 'effective' for this purpose were unknown. It was reasonable to use a representative set of variables. DTMs of the following local topographic attributes were derived from the smoothed DEMs: twelve curvatures (i.e. horizontal, vertical, accumulation, difference, ring, minimal, maximal, mean, Gaussian, unsphericity, horizontal excess, and vertical excess curvatures), slope steepness, slope aspect, rotor, and a model of accumulation zones. DTMs of two regional topographic variables were derived from the smoothed DEMs: specific catchment area and specific dispersive area. Definitions, formulae, and interpretations of the variables can be found elsewhere (Shary *et al.* 2002). Local variables were calculated by the method designed for a spheroidal trapezoidal grid (Florinsky 1998b). Regional variables were derived by a single flow direction algorithm including preliminary filling of sinks (Martz and de Jong 1988) adapted to a spheroidal trapezoidal grid.

The parameters of the Krassovsky ellipsoid, as well as formulae for lengths of meridian and parallel arcs and area of a spheroidal trapezium (Morozov 1979), were employed to calculate changing sizes and area of a spheroidal trapezoidal moving window (Florinsky 1998b) during the DEM smoothing and the derivation of topographic variables. The DEM was processed as a virtually closed spheroidal matrix of elevation values. As a result, there was not the usual loss of border columns and rows due to the application of moving windows. All DTMs produced had a resolution of 30 arc-minutes, and consisted of 721 columns by 361 rows.

To gain a better representation and understanding of global patterns of topographic attributes (Figure 2), their values were transformed as follows (Shary *et al.* 2002):

$$T' = \operatorname{sign}(T) \cdot \ln(1 + 10^m |T|), \qquad (1)$$

where T is an attribute, $m = 0$ for slope steepness, aspect, and regional variables, $m = 16$ for accumulation, ring, and Gaussian curvatures, and $m = 9$ for other variables. Specific catchment and dispersive areas were also mapped classifying their values into two levels (Figure 3). The Plate

Carrée projection was used to map topographic variables. DTM treatment was accomplished with LandLord 4.0 (Florinsky *et al.* 1995).

Maps of topographic variables were visually examined in detail. Attention was paid to lineaments running over the entire globe or a hemisphere. Contrary to many lineaments of regional and continental scales, global lineaments are not manifested as uninterrupted linear patterns of the map image or sequences of such lines. A global lineament may be visually detected due to traits of the image *texture* strung out along some direction along a line running over the Earth (Figure 4). Structures detected were mapped using the Plate Carrée projection for the entire Earth, and polar stereographic projections for the Northern and Southern hemispheres (Figure 5) with ArcView GIS 3.0 (© ESRI, 1992–1996).

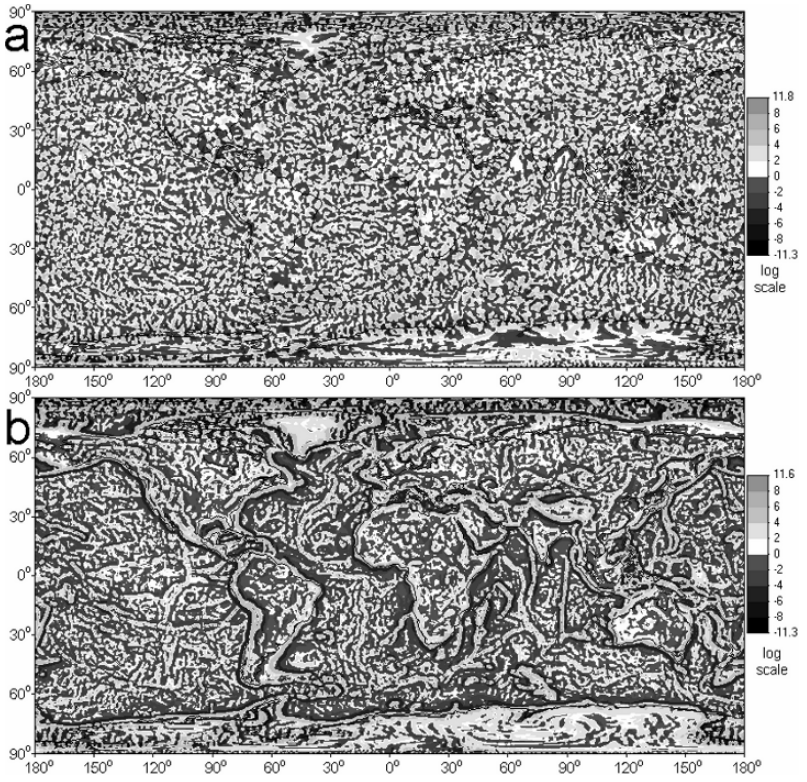

Figure 2 (a-b). Global maps of topographic variables derived from the 3-times smoothed DEM. (a) Horizontal curvature. (b) Vertical curvature.

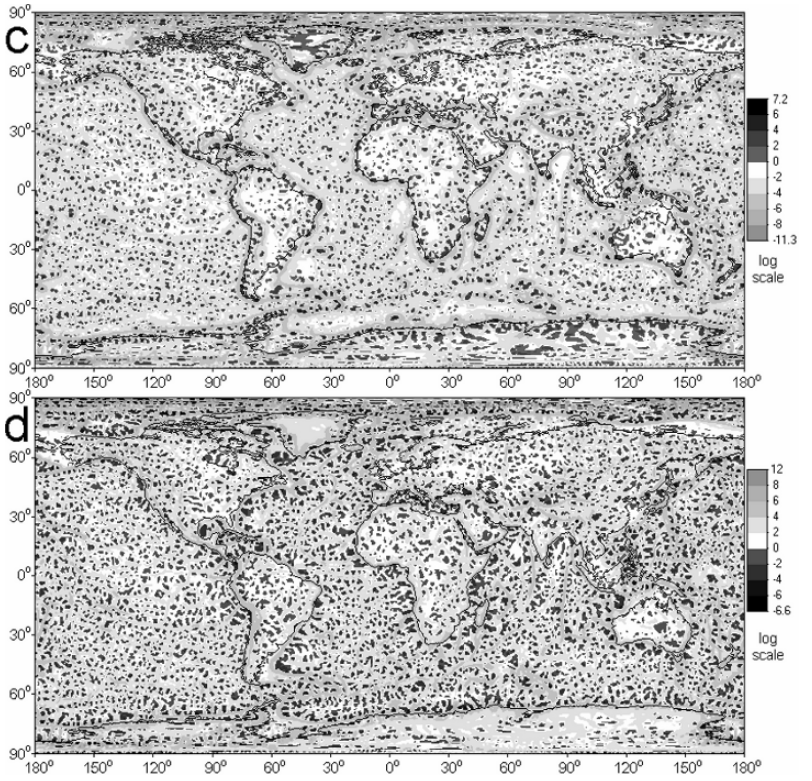

Figure 2 (c-d). Global maps of topographic variables derived from the 3-times smoothed DEM. (c) Minimal curvature. (d) Maximal curvature.

3 Results and Discussion

Global maps of topographic variables represent peculiarities of the Earth's mega-relief in different ways, according to the physical and mathematical sense of a particular variable. For example, horizontal curvature (Figure 2a) delineates areas of flow divergence and convergence (positive and negative values, respectively. These areas correspond to spurs of valleys and ridges (dark and light coloured patterns of the map image, respectively), which form so-called flow structures. At this generalization level, flow structures are most pronounced in ocean basins. Vertical curvature (Figure 2b) is a measure of relative acceleration and deceleration of flows (positive and negative values, respectively). Among other features, the map of vertical curvature shows 'mega-scarps', such as edges of continents and mountains. Low negative values of minimal curvature delineate

valleys and troughs, while positive values delineate ‘mega-hills’ (Figure 2c). High positive values of maximal curvature show ridges, while negative values show ‘mega-depressions’ (Figure 2d). Catchment area measures an upslope area, which is potentially drained through a given point on the land surface. At the global scale, low values of specific catchment area (Figure 2e) delineate land and oceanic ridges as black lines (e.g. the Andes, Alps, mid-ocean ridges), while its high values show land and oceanic valleys as white lines and depressions as light coloured areas (e.g. the Mediterranean Sea, Gulf of Mexico, Angola Basin). Dispersive area measures a downslope area, which may be potentially exposed by flows passing through a given point on the land surface. At this generalization level, high values of specific dispersive area (Figure 2f) delineate mountain systems and highlands as light coloured areas (e.g. the Himalayas, Urals, Ethiopian Highlands) as well as land and oceanic ridges as white lines.

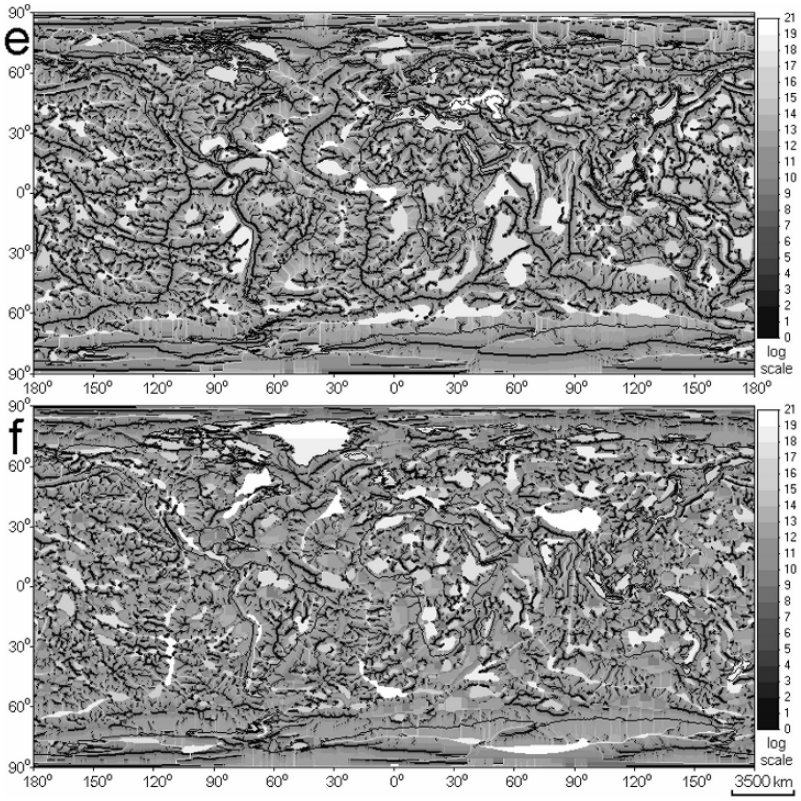

Figure 2 (e-f). Global maps of topographic variables derived from the 3-times smoothed DEM. (e) Specific catchment area. (f) Specific dispersive area.

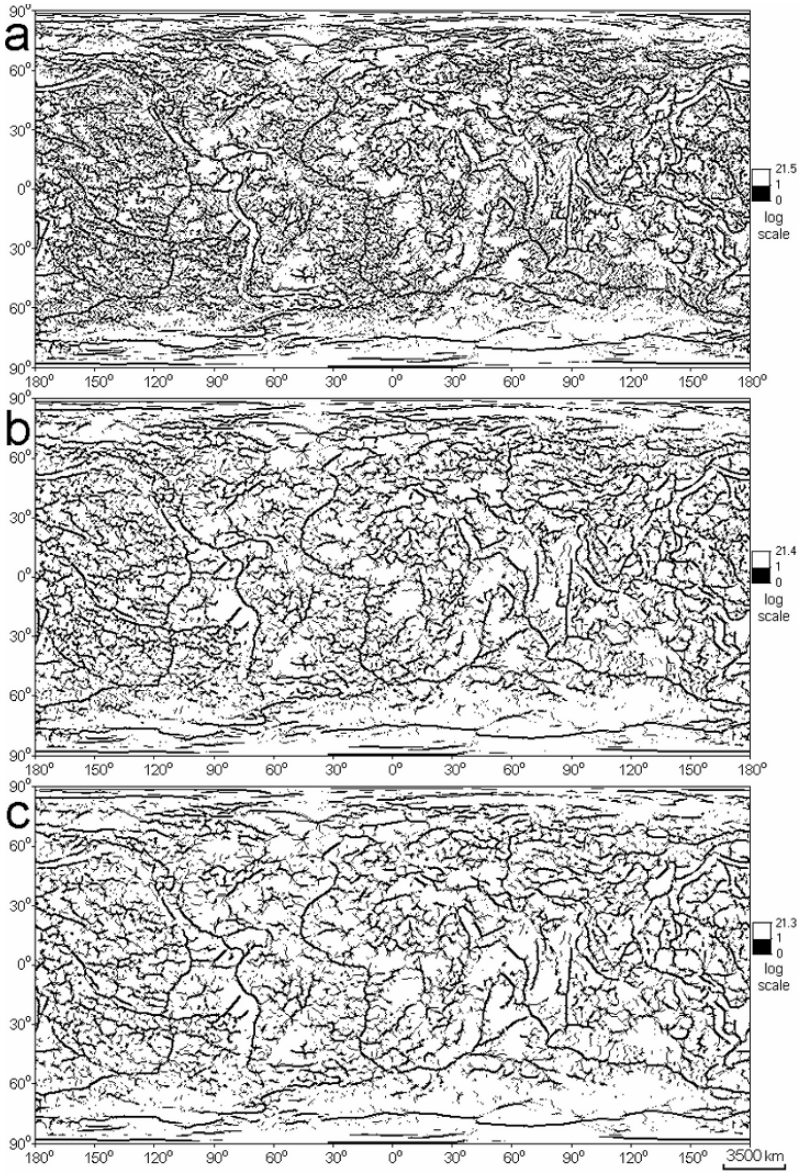

Figure 3. Global maps of catchment area classified into two levels. (a) 1-time smoothing. (b) 2-times smoothing. (c) 3-times smoothing.

Maps of specific catchment area with values classified into two levels (Figure 3) were best suited to detect global lineaments. These maps display the ridge network of the planet. The greater the number of DEM smoothing, the more generalized picture of the network is mapped. Analysing

these maps (Figure 4), it was possible to detect five mutually symmetrical pairs of global lineaments, viz. five double helices encircling the Earth from pole to pole (Figure 5). The structures revealed are helical zones rather than simply lines. Each double helix is named after the area(s) of intersection(s) of its arms (Table 1). Arms running clockwise upward and counter-clockwise upward (dextral and sinistral helices) are called right and left arms, respectively. Each helical zone transgresses plate boundaries and regions dissimilar in respect to their tectonic origin, rock composition, and age.

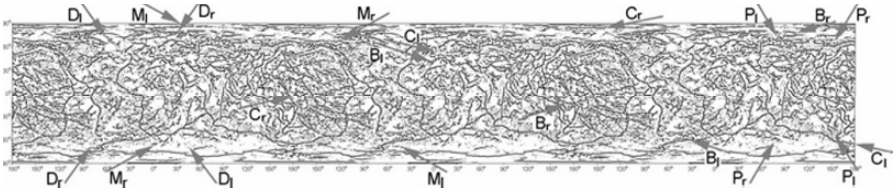

Figure 4. Visual detection of global helical structures on the three-fold map of specific catchment area derived from the 2-times smoothed DEM. Ten pairs of arrows show proposed positions of ten helical arms. Structures are indicated by labels: C = Caucasus-Clipperton, B = Biscay-Santa Cruz, M = Marcus, D = Dakar, and P = Palawan. Subscripts: r = right arm, l = left arm.

The global lineaments revealed cannot be artefacts due to DEM errors, the DEM treatment, or the DEM grid geometry (Florinsky 2005). First, noise and errors usually have a random distribution in DEMs. Second, smoothing and derivation of topographic variables were carried out using local filters (n × n moving windows). Third, the grid geometry may amplify its own preferential directions: orthogonal (north-south, east-west) and diagonal (northeast-southwest, northwest-southeast). However, the structures detected have (a) the global character relative to the DEM; and (b) directions distinct from orthogonal and diagonal ones. The subjective character of a visual analysis remains the only cause of possible artefacts.

Notice that some visually recognizable artefacts are typical for Polar Regions on all maps produced (Figures 2 and 3). They were caused by too low accuracy of initial cartographic sources used to compile the related portions of ETOPO2 and GLOBO. There are also computational artefacts on maps of specific catchment and dispersive areas, which are manifested as straight parallel lines located predominantly in the Polar Regions (Figure 2e, f). They are well known artefacts of single flow direction algorithms common for flat slopes. However, the artefacts did not influence the detection of global helical structures since the artefacts are situated within limited zones of the maps.

Table 1. Parameters of the global topographic helices.

Structure	Left arm		Right arm		Geograph-ical coordinates of the arm intersec-tion(s)
	Lengths (km)	Inclination at the equa-tor (°)	Lengths (km)	Inclination at the equator (°)	
Caucasus-Clipperton	55,800	167.5	31,500	12.5	46.4°N, 44.81°E; 5.9°N, 134.7°W
Biscay-Santa Cruz	39,600	162.2	29,800	17.5	44.4°N, 7.3°W; 12.9°S, 171.4°E
Marcus	26,500	150.6	24,900	29.7	21.4°N, 157.5°E
Dakar	17,700	126.9	17,200	53.3	14.9°N, 16.0°W
Palawan	15,400	121.3	15,300	59.5	9.9°N, 119.1°E

The Caucasus-Clipperton double helix (Figure 5a) coincides with one of the structures reported by Volkov (1995) (Figure 1c). The left arm of the Biscay-Santa Cruz structure (Figure 5b) partly agrees with the left arm of one of the helices detected by O'Driscoll (1980) (Figure 1b). A comparison of inclination angles of theoretical traces of torsional deformation (Section 1, Figure 1a), and that of the double helices revealed (Table 1) shows that the Caucasus-Clipperton and Biscay-Santa Cruz structures can be assigned to traces of shear fractures, while the Dakar and Palawan structures can be assigned to traces of cleavage cracks. The mean deviation of inclination angles of the structures from the theoretical values is 2.8°. Of the five double helical structures detected, four have inclination angles fitting theoretical values. This suggests that one may consider topographically expressed helical structures as fracture traces of global torsion. There are several deviations from the theory, such as: (a) arms of each double helix meet off the equator; and (b) there is the Marcus double helix with 'abnormal' inclination. The discrepancies might be in part attributed to the deviation of the Earth's shape from a sphere, as assumed in the model of Rance (1968).

The polar stereographic map of the Northern hemisphere presents the Caucasus-Clipperton structure (Figure 5a) as a nearly ideal plane two-arm Archimedean spiral (Fikhtengolts 1966, p. 520). Away from the pole, it is approximated by the equation:

$$r = a\theta \tag{2}$$

where r is a radius, θ is an angle, and a is a constant; $a = 1.01$. The left arm of this structure is explicitly described as a spherical Archimedean spiral (Klíma *et al.* 1981):

$$\sigma = R\psi_0\lambda/(2\pi) \tag{3}$$

where σ is a length of a meridian arc between the pole and a point on the spiral (ψ, λ), R is a radius of the sphere, ψ_0 is a value by which ψ changes if λ changes by 2π, $\psi = 0.5\pi - \varphi$, φ is the latitude, and λ is the longitude; ψ_0 = 79.55°. Volkov (2006, personal communication) supposed that all lineaments delineated by him (Figure 1c) are spherical Archimedean spirals. This issue needs further investigation.

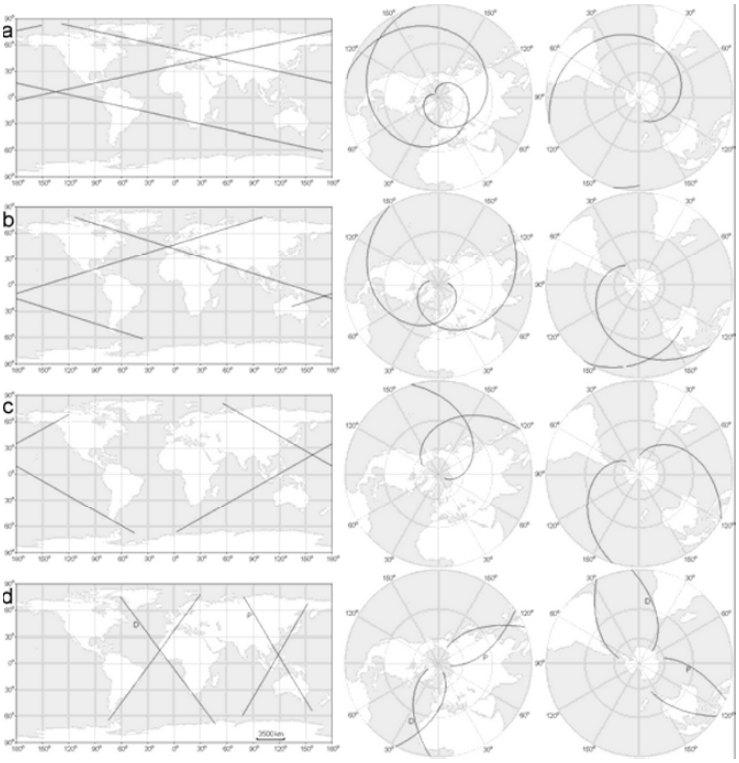

Figure 5. Double helical structures for the entire Earth and the Northern and Southern hemispheres. (a) Caucasus-Clipperton. (b) Biscay-Santa Cruz. (c) Marcus. (d) Dakar (D) and Palawan (P).

Literature provides evidence for shears and increased fracturing along double helices. In particular, the left arm of the Caucasus-Clipperton structure (Figure 5a) within Europe was associated with a strike-slip fault system (Moody 1966). Within the Pacific Ocean basin, the left arm of the Biscay-Santa Cruz structure (Figure 5b) was also interpreted as a system of strike-slip faults (Moody 1966). This helix is coaxial with a zone of planetary

fracturing within Eurasia (Miroshnichenko *et al.* 1984). Along this zone, there is a belt of intensive rock fracturing 3,000 km wide, including right-lateral strike-slip faults along the northern border of the belt (Poletaev 1986). Relatively small strike-slip faults southward of Madagascar and northward of New Guinea (Moody 1966) seem to be parts of the right arm of the Marcus structure (Figure 5c). Fragments of the right arm of the Dakar structure (Figure 5d) were associated with shear systems (Vening Meinesz 1947), strike-slip faults (Moody 1966), and fracture zones (Miroshnichenko *et al.* 1984). The left arm of the Dakar double helix is coaxial with a zone of planetary fracturing (Miroshnichenko *et al.* 1984). Between Indonesia and the Philippines, a fragment of the right arm of the Palawan double helix (Figure 5d) was interpreted as a system of strike-slip faults (Chebanenko 1963, Moody 1966). In Australia, the left arm of the Palawan structure and the right arm of the Biscay-Santa Cruz structure were also associated with strike-slip faults (Chebanenko 1963).

Intensive crystallo- and metallogeny are observed along both arms of the Caucasus-Clipperton helix (Figure 5a). Evseev (1989) reported finds of large crystals of viterite and strontianite along a line coaxial with the left arm of the structure in Europe, from Scotland to the Caspian Sea. Along the right arm of the structure in Siberia, between 70°E and 170°W, there were numerous finds of unique large crystals including amethyst, aquamarine, axinite, azurite, beryl, calomel, calcite, charoite, diopside, fluorite, garnet, hematite, magnetite, pegmatite, smoky and green quartz, spinel, spherulite, topaz, tourmaline, etc. (Evseev 1993). Large iron and gold ore deposits of endogenic and metamorphic origin are located along both arms of this helix in Eurasia, Central and South America (Volkov 1995). It is common knowledge that lineaments of the regional and continental scales may control ore deposits since an increased fracturing of the crust along lineaments, especially at sites of their intersection, is favourable to magmatic intrusions (Favorskaya 1977, O'Driscoll 1986). This may explain the occurrence of crystal and ore deposits along helical structures.

Global helical topographic structures are not unique to the Earth. Slyuta *et al.* (1989) discovered a dense, regular network of dextral and sinistral spiral structures on radar scenes of the Northern hemisphere of Venus (Figure 6). These planetary structures are wound around the axis of rotation of Venus. They are topographically manifested as troughs, scarps, and depressions. Slyuta *et al.* (1989) believed that strong rotational forces had formed the network during the deceleration of Venus's rotation. They suggested that the helical network is a relict feature, an 'imprint' of ancient rotational stress fields, because the current rotation velocity of Venus is quite slow. The low intensity of erosion has allowed relict helical structures to persist on the Venusian surface. This author supposes that double helices

of the Earth are also relict features. Strong erosion led to their hidden manifestation in modern topography (Figure 4).

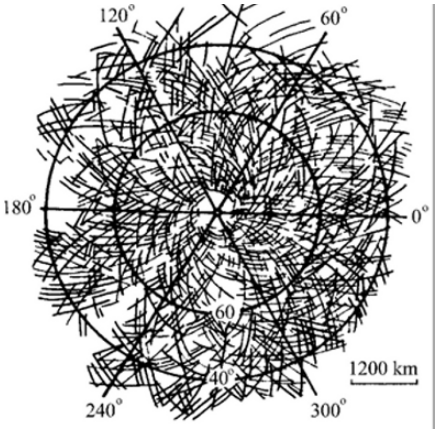

Figure 6. Spiral structures of the Northern hemisphere of Venus (after Slyuta et al. 1989, Figure 2, © Plenum Publishing Corporation, 1990; reproduced with kind permission of Springer Science and Business Media).

Contrary to regional lineaments and some structures of the continental scale clearly recognizable on the maps of specific catchment area (e.g. mountain chains, mid-ocean ridges, and ocean troughs), double helical structures are not in harmony with the plate-tectonic theory. Notice that the existence of transcontinental and planetary lineaments was one of the main geological and geomorphic facts contradicting the plate-tectonic ideas (Favorskaya 1977, Pavlenkova 1995, Pratt 2000, Smoot 2001). To link these facts with possible continental drift, seafloor spreading, and subduction, some modifications of the plate-tectonic hypothesis have been proposed. For instance, Moody (1966) proposed that continental drift is a movement of crustal blocks along major lineament zones with relatively stable mantle roots. Besprozvanny *et al.* (1994) suggested that regularities in the global lineament network are caused by dissipative structures of the upper core. Once again, our results set one to think about a tectonic paradigm more adequately depicting the actual structure and evolution of the Earth.

4 Conclusions

The application of digital terrain modelling provided support for the hypothesis for the existence of double helical structures of the Earth, which are topographically expressed and possibly associated with the torsional deformation of the planet. To understand fully the origin and properties of helical structures, comprehensive studies should be conducted. A quantitative

analysis of the global topography may be essential to give a clearer insight into the planetary evolution.

Eighteen topographic variables were for the first time calculated and mapped for the entire surface of the Earth, including both land and seafloor topography. To produce readable and interpretable global maps of topographic attributes, DEM denoising was the key step in data processing. This paper focused on lineaments, but global maps of topographic variables can be useful to study other problems of tectonics and geophysics (ring structures, lithospheric strain, etc.). These maps can be integrated into virtual geological and geomorphic globes (Rundquist *et al*. 2002, Tooth 2006).

Acknowledgements

The author thanks V.G. Trifonov (Geological Institute, Russian Academy of Sciences, Moscow, Russia), A.E. Fedorov (Annual Seminar 'The System of the Planet Earth: Non-Conventional Problems of Geology', Moscow, Russia), Yu.V. Volkov (Research Computing Center, M.V. Lomonosov Moscow State University, Moscow, Russia), and H. Rance (Queensborough Community College, City University of New York, Bayside, USA) for discussions, as well as P.A. Shary (Institute of Physical, Chemical, and Biological Problems of Soil Science, Russian Academy of Sciences, Pushchino, Russia), G. Ventura (Istituto Nazionale di Geofisica e Vulcanologia, Roma, Italy), and an anonymous referee for useful criticism. The study was partly supported by RFBR grant 06-05-74882.

References

Arabelos, D., (2000), Intercomparisons of the global DTMs ETOPO5, Terrain-Base and JGP95E, *Physics and Chemistry of the Earth (A)*, **25**: 89–93.

Besprozvanny, P.A., Borodzich, E.V. and Bush, V.A., (1994), Numerical analysis of ordering relations in the global network of lineaments, *Physics of the Solid Earth*, **30**: 150–159.

Cazenave, A., Souriau, A. and Dominh, K., (1989), Global coupling of Earth surface topography with hotspots, geoid and mantle heterogeneities, *Nature*, **340**: 54–57.

Chebanenko, I.I., (1963), Principal Regularities of Fault Tectonics of the Earth's Crust and Its Problems, Kiev: Ukrainian Academic Press (in Russian).

Chebanenko, I.I. and Fedorin, Ya.V., (1983), On a new type of rotation-tectonic lines in the Earth's lithosphere, *Doklady Akademii Nauk SSSR*, 270: 406–409 (in Russian).

Cherednichenko, A.I., Burmistenko, V.M., Tokovenko, V.S. and Chebanenko, I.I., (1966), Attempt of laboratory simulation of planetary faults (lineaments) of the Earth, *Dopovidi Academii Nauk Ukrainy*, 10: 1333–1336 (in Ukrainian, with English abstract).

Chorowicz, J., Dhont, D. and Gündoğdu, N., (1999), Neotectonics in the eastern North Anatolian fault region (Turkey) advocates crustal extension: mapping from SAR ERS imagery and digital elevation model, *Journal of Structural Geology*, **21**: 511–532.

Coe, M.T., (1998), A linked global model of terrestrial hydrologic processes: simulation of modern rivers, lakes, and wetlands, *Journal of Geophysical Research*, **D103**: 8885–8899.

Dolitsky, A.V. and Kiyko, I.A., (1963), On causes of deformation of the Earth's crust, In Nalivkin, D.V. and Tupitsin, N.V. (eds.): *Problems of Planetary Geology,* Moscow: Gosgeoltekhizdat: 291–312 (in Russian).

Evseev, A.A., (1989), Regularity in the distribution of discoveries of large crystals, *New Data on Minerals*, **36**: 53–67 (in Russian).

Evseev, A.A., (1993), Siberia's crystals and symmetry in the distribution of occurrences of minerals, *World of Stones*, 1: 11–20.

Favorskaya, M., (1977), Metallogeny of deep lineaments and new global tectonics, *Mineralium Deposita*, **12**: 163–169.

Fikhtengolts, G.M., (1966), A Course in Differential and Integral Calculus, Vol. 1, 6th ed., Moscow: Nauka (in Russian).

Florinsky, I.V., (1996), Quantitative topographic method of fault morphology recognition, *Geomorphology*, **16**: 103–119.

Florinsky, I.V., (1998a), Combined analysis of digital terrain models and remotely sensed data in landscape investigations, *Progress in Physical Geography*, **22**: 33–60.

Florinsky, I.V., (1998b), Derivation of topographic variables from a digital elevation model given by a spheroidal trapezoidal grid, *International Journal of Geographical Information Science*, **12**: 829–852.

Florinsky, I.V., (2002), Errors of signal processing in digital terrain modelling, *International Journal of Geographical Information Science*, **16**: 475–501.

Florinsky, I.V., (2005), Artificial lineaments in digital terrain modelling: can operators of topographic variables cause them? *Mathematical Geology*, **37**: 357–372.

Florinsky, I.V., Grokhlina, T.I. and Mikhailova, N.L., (1995), LANDLORD 2.0: the software for analysis and mapping of geometrical characteristics of relief, *Geodezia i Cartografia*, 5: 46–51 (in Russian).

GLOBE Task Team, (1999), *The global land one-kilometer base elevation (GLOBE) digital elevation model, version 1.0,* Boulder: NOAA, National Geophysical Data Center, Available online at: http://www.ngdc.noaa.gov/mgg/topo/globe.html (accessed 22 October 2005).

Hastings, D.A. and Dunbar, P.K., (1998), Development and assessment of the global land one-km base elevation digital elevation model (GLOBE), *ISPRS Archives*, **32**: 218–221.

Hobbs, W.H., (1904), Lineaments of Atlantic Border region, *Geological Society of America Bulletin*, **15**: 483–506.

Katterfeld, G.N. and Charushin, G.V., (1973), General grid systems of planets, *Modern Geology*, **4**: 253–287.

Kazanskii, B.A., (2005), Calculation of the Earth's topography-related potential energy from digital data, *Izvestiya, Physics of the Solid Earth*, **41**: 1023–1026.

Klíma, K., Pick, M. and Pros, Z., (1981), On the problem of equal area block on a sphere, *Studia Geophysica et Geodaetica*, **25**: 24–35.

Knetsch, G., (1965), Über ein Structur-Experiment an einer Kugel und Beziehungen zwischen Gross-Lineamenten und Pol-Lagen in der Erdeschichte, *Geologische Rundschau*, **54**: 523–548.

Makarov, V.I., (1981), Lineaments: problems and trends of studies by remote sensing techniques, *Izvestiya Vuzov, Geologia i Razvedka*, 4: 109–115 (in Russian).

Martz, L.W. and de Jong, E., (1988), CATCH: a Fortran program for measuring catchment area from digital elevation models, *Computers and Geosciences*, **14**: 627–640.

McClean, C.J. and Evans, I.S., (2000), Apparent fractal dimensions from continental scale digital elevation models using variogram methods, *Transactions in GIS*, **4**: 361–378.

Miroshnichenko, V.P., Berezkina, L.I. and Leontieva, E.V., (1984), *Planetary Fracturing of Sedimentary Cover of the Lithosphere from Remotely Sensed Data*, Leningrad: Nedra (in Russian).

Moody, J.D., (1966), Crustal shear patterns and orogenesis, *Tectonophysics*, **3**: 479–522.

Mooney, W., Laske, G. and Master, T., (1998), CRUST 5.1: A global crustal model at 5x5, *Journal of Geophysical Research*, **B103**: 727–747.

Moore, I.D., Grayson, R.B. and Ladson, A.R., (1991), Digital terrain modelling: a review of hydrological, geomorphological and biological applications, *Hydrological Processes*, **5**: 3–30.

Moore, R.F. and Simpson, C.J., (1983), Image analysis – a new aid in morphotectonic studies. In *17th International Symposium on Remote Sensing of Environment*, 9–13 May 1983, Ann Arbor, USA, Vol. 3, Ann Arbor: Environmental Research Institute of Michigan: 991–1002.

Morozov, V.P., (1979), *A Course in Spheroidal Geodesy. 2nd enl. and rev. ed.*, Moscow: Nedra (in Russian).

O'Driscoll, E.S.T., (1980), The double helix in global tectonics, *Tectonophysics*, **63**: 397–417.

O'Driscoll, E.S.T., (1986), Observations of the lineament–ore relation, Philosophical Transactions of the Royal Society of London, Series A: Mathematical and Physical Sciences, **317**: 195–218.

O'Leary, D.W., Friedman, J.D. and Pohn, H.A., (1976), Lineament, linear, lineation: some proposed new standards for old terms, *Geological Society of America Bulletin*, **87**: 1463–1469.

Pavlenkova, N.I., (1995), Structural regularities in the lithosphere of continents and plate tectonics, *Tectonophysics*, **243**: 223–229.

Poletaev, A.I., (1986), *Seismotectonics of the Main Kopetdag Fault Zone*, Moscow: Nauka (in Russian).

Pratt, D., (2000), Plate tectonics: a paradigm under threat, *Journal of Scientific Exploration*, **14**: 307–352.

Rance, H., (1967), Major lineaments and torsional deformation of the Earth, *Journal of Geophysical Research*, **72**: 2213–2217.

Rance, H., (1968), Plastic flow and fracture in a torsionally stressed planetary sphere, *Journal of Mathematics and Mechanics*, **17**: 953–974.

Rance, H., (1969), Lineaments and torsional deformation of the Earth: Indian Ocean, *Journal of Geophysical Research*, **74**: 3271–3272.

Renssen, H. and Knoop, J.M., (2000), A global river routing network for use in hydrological modelling, *Journal of Hydrology*, **230**: 230–243.

Rundquist, D.V., Ryakhovsky, V.M., Gatinsky, Yu.G. and Chesalova, E.I., (2002), GIS-project 'The geodynamic globe, scale 1:10,000,000' for global monitoring of various geological processes, *Proceedings of the All-Russian Scientific Conference 'Geology, Geochemistry, and Geophysics on the Boundary of the 20th and 21st Centuries'*, 8–10 Oct. 2002, Moscow, Russia, Vol. 1 ,Moscow: Svyaz-Print: 87–88 (in Russian).

Schowengerdt, R.A. and Glass, C.E., (1983), Digitally processed topographic data for regional tectonic evaluations*, Geological Society of America Bulletin*, **94**: 549–556.

Shary, P.A., Sharaya, L.S. and Mitusov, A.V., (2002), Fundamental quantitative methods of land surface analysis, *Geoderma*, **107**: 1–32.

Slyuta, E.N., Kudrin, L.V. and Sinilo, V.P., (1989), Preliminary data on the nature of a planetary system of lineaments observed in radar images of Venus (data from Venera-15 and -16), *Cosmic Research*, **27**: 786–797.

Smoot, N.C., (2001), Earth geodynamic hypotheses updated, *Journal of Scientific Exploration*, **15**: 465–494.

Tooth, S., (2006), Virtual globes: A catalyst for the re-enchantment of geomorphology? *Earth Surface Processes and Landforms*, **31**: 1192–1194.

U.S. Department of Commerce, NOAA, National Geophysical Data Center, (2001), *2–minute gridded global relief data (ETOPO2),* Available online at: http://www.ngdc.noaa.gov/mgg/fliers/01mgg04.html (accessed 21 October 2005).

Vening Meinesz, F.A., (1947), Shear patterns of the Earth's crust, *Transactions of the American Geophysical Union*, **28**: 1–61.

Volkov, Y.V., (1995), Loxodromy and minerageny (the influence of astronomic resonances in the Earth-Moon system on the origin of ore deposits in the Earth's crust), *Bulletin of Moscow Society of Naturalists, Geological Series*, **(70)**6: 90–94 (in Russian, with English abstract).

Vörösmarty, C.J., Fekete, B.M., Meybeck, M. and Lammers, R.B., (2000), Geomorphometric attributes of the global system of rivers at 30-minute spatial resolution*, Journal of Hydrology*, **237**: 17–39.

http://www.springer.com/978-3-540-77799-1

Advances in Digital Terrain Analysis

(Eds.)Q. Zhou; B. Lees; G.-a. Tang
2008, XIV, 462 p. 183 illus., Hardcover
ISBN: 978-3-540-77799-1